This is a repository copy of *Experimental study on hybrid precast tunnel segments reinforced by macro-synthetic fibres and glass fibre reinforced polymer bars*.

White Rose Research Online URL for this paper:
https://eprints.whiterose.ac.uk/171687/

Version: Accepted Version

1   **Experimental study on hybrid precast tunnel segments reinforced by macro-synthetic fibres and glass fibre reinforced**

2   **polymer bars**

3   **O. Tengilimoglu [a], U. Akyuz [b]**

4   *[a] Institute for Transport Studies, University of Leeds, Leeds, United Kingdom*

5   *[b] Department of Civil Engineering, Middle East Technical University, Ankara, Turkey*

6   Corresponding authors.

7   E-mail address: ts18ot@leeds.ac.uk (O. Tengilimoglu), han@metu.edu.tr (U. Akyuz).

8   Postal address: Institute for Transport Studies, 34-40 University Road, University of Leeds, Leeds LS2 9JT (O. Tengilimoglu),

9   Dept. of Civil Engineering, K2 Building, Room 204, Middle East Technical University, 06800 Ankara, Turkey (U. Akyuz)

10

11   **ABSTRACT**: Increasing the popularity of using fibres in precast structures has brought questions about their usability in

12   segmental tunnel linings as an alternative to the conventional reinforced lining. Most prior studies have already revealed that

13   the replacement of conventional steel reinforcement is possible with steel fibres. However, the usability of macro-synthetic

14   fibres (MSFs) as reinforcements in precast tunnel segments is still unclear and one of the controversial questions to be answered.

15   This study aims to evaluate the structural applicability of using polypropylene (PP) MSFs in precast tunnel segments by means

16   of an experimental program on full-scale specimens. Within this framework, totally fourteen full-scale precast tunnel segments

17   of Mecidiyekoy - Mahmutbey underground railway tunnel in Istanbul/Turkey characterized by four different reinforcement

18   cases were analysed: i) typical conventional steel reinforcement; ii) the combination of MSFs and conventional reinforcement;

19   iii) the combination of MSFs and glass fibre reinforced polymer (GFRP) rebars; and iv) MSFs only. Flexural tests were carried

20   out to compare the flexural behaviour of specimens at the allowable crack opening width, while point load tests were conducted

21   to observe the structural performance of precast tunnel segments under the effect of design thrust forces. The experimental

22   results showed that the combination of MSFs and GFRP could be an innovative solution for precast tunnel segments in case of

23   using a suitable quantity that satisfied the project requirements. Although PP fibres exhibited adequate spalling and splitting

24   stress control, it is observed that they could not overcome high flexure forces without using reinforcement bars at a low volume

25   of fractions. Thus, more comprehensive studies need to perform on GFRP + MSFs segments because of having the advantages

26   of corrosion resistance in the presence of an aggressive surrounding environment.

27   **Keywords**: Full-Scale Tests, Precast Tunnel Segments, Macro-Synthetic Fibres, Glass Fibre Reinforced Polymer Rebars

28   **1. Introduction**

29   With the advancements of the tunnel construction technology and adoption of more powerful Tunnel Boring Machines

30   (TBMs), the popularity of precast tunnel segmental lining in metropolitan areas has increased dramatically in the last decades

31   (Conforti et al., 2017). Precast tunnel segmental linings serve as both initial ground support and final lining in the modern

32   tunnels, which are constructed by full-face mechanised excavation methods (Bakhshi and Nasri, 2015) and they provide the

required operational cross-sections for many projects such as water supply, wastewater, gas pipeline, railways, and power cable. However, there are some drawbacks in terms of structural performance and manufacturing process of precast tunnel lining. The bended shape of the tunnel segments causes the use of conventional steel reinforcements with complex detailing (Caratelli et al., 2011). This result in increases in project construction time and higher labour costs due to requiring extra manpower during the manufacturing process. Moreover, in tunnels reinforced by conventional steel reinforcements, corrosion can be a problem for precast tunnel segments especially, in harsh soil environment and damaged part of the tunnel. In general, to prevent the possible corrosion on steel reinforcing bars, cathodic protection is applied in tunnel lining, but this application leads to an increase in project cost. Therefore, one of the main efforts of engineers is to decrease the construction time and enhance the structural behaviour of precast tunnel segments in terms of flexural bearing capacity, corrosion resistance, and crack control.

Fibre reinforced concretes (FRC) are popularly tried to be used for the construction of tunnel lining since they allow the possibility of reduction or disuse in conventional rebars. In the last decade, various experimental and numerical studies have been conducted to investigate the usability of FRC in tunnels (Plizzari and Tiberti, 2008; Caratelli et al., 2011; Beno and Hilar, 2013; Abbas et al., 2014a; Liao et al., 2015; Di Carlo et al., 2016; Gong et al., 2017) and some authors conducted research on actual applications (Molins and Arnau, 2011; Caratelli et al., 2012; De La Fuente et al., 2012). In these efforts, steel fibres reinforced concretes were commonly investigated for the adoption in tunnels and they are successfully used in many tunnel projects across the world (ITA report n.16, 2016). However, segments reinforced with steel fibres require additional measures in terms of crack width and cover thickness, as they are expected to be exposed to corrosion in an aggressive environment (Abbas and Nehdi, 2018; ITATech report n.7, 2016). More importantly, cathodic protection of steel fibres is harder than conventional reinforcements due to the discontinuity. For this reason, there is a growing interest in the field of engineering on macro-synthetic fibres (MSFs) to obtain more durable precast tunnel segments due to its higher resistance to corrosion than steel fibres (Yan et al., 2015; Conforti et al., 2017; Demir, 2019). However, to date, limited studies have been conducted to investigate the structural behaviour of segments reinforced with synthetic fibres. Previous research revealed that the usability of polypropylene MSFs is possible in a hydraulic tunnel (Conforti et al., 2017), but it is controversial whether they are suitable for relatively large metro tunnels. More interestingly, although synthetic fibres have been used in some tunnels in the last decade (ITA report n.16, 2016), quite limited experimental research has been done associated with MSFs in metro tunnel segments in the literature. Recently, Conforti et al., (2019) investigated the probability of total or partial replacement of conventional reinforcement in the metro tunnel lining with the help of using MSFs. Based on their experimental research, they revealed that using MSFs can be a very effective solution in combination with traditional steel rebars to withstand the main stresses that arise in a segment both construction and final phases. They conclude that the advantages of the hybrid system in improving the flexural performances, increasing the ductility level, and reducing the crack widths.

More recently, in addition to MSFs, the possibility of implementation of glass fibre reinforced polymers (GFRP) rebars in tunnel segments were investigated by some authors with the help of experimental methods on full-scale specimens (Caratelli et al., 2016; Caratelli et al., 2017; Spagnuolo et al., 2017, Meda et al., 2019). The findings of these studies demonstrated that

2

using GFRP rebars instead of conventional steel reinforcements in precast tunnel segments are possible and allows many advantages in the sense of structural durability. The main benefits of the GFRP reinforcing bars are their high tensile strength and being non-corrosive properties. Furthermore, compared to other types of fibre reinforced polymer (FRP) bars, GFRP materials do not conduct the electricity and they are non-magnetic (ACI 440.1R-15, 2015). Nevertheless, using GPFR reinforcing bars in concrete also has some handicaps in terms of structural performance and there is a need for extra attention since they cannot be suitable for all type of applications (Meda et al., 2019). GFRP rebars face a static fatigue problem when they are subjected to high-level long-term tensile stresses (Almusallam et al., 2006) and have an anisotropic property which the coefficient of thermal expansion differs in longitudinal and radial directions. This also affects the shear strength capacity of GFRP rebar which is lower than steel reinforcement. Another critical factor is that concrete structures reinforced with GFRP bars have low ductility since they show linear elastic behaviour up to failure. Moreover, serviceability has to be controlled during the design part of the structure because of the lower modulus of elasticity of GFRP bars and they show poor bond behaviour with respect to the traditional steel reinforcement (Yoo et al., 2015; Yan et al., 2016).

From the structural point of view, GFRP rebars do not suffer corrosion problems, this is extremely important for tunnels passing through aggressive soil conditions. Therefore, for the purpose of removing the cathodic protection in the tunnel and reducing project cost, macro-synthetics fibres and GFRP rebars can be used in precast tunnel segment together as a hybrid solution. However, up to the present, there is scant evidence on the usability of GFRP rebars with synthetic fibres in tunnel segments as a hybrid solution. Within this framework, experimental programs on fourteen full-scale segments of Mecidiyekoy – Mahmutbey (MM) metro tunnel (Istanbul) were carried out to investigate the possibility of using PP macro-synthetic fibres with or without rebars in precast tunnel segments and also to evaluate the usability of glass fibre reinforced polymer (GFRP) reinforcing bars instead of conventional bars in precast tunnel segments. This research aims to enhance the structural performance of precast tunnel segments and to reduce the construction time by using PP fibres in precast tunnel segments. Additionally, the research work presented herein contributes to the existing gap in the literature by using MSFs along with GFRP rebars in precast tunnel segments, which enable exclusion of the cathodic protection in tunnels.

2. Full-Scale Experimental programme

2.1 Geometry and reinforcement details of specimens

The MM metro line project that is located within the European side of Istanbul city comprised of the construction of a twin tunnel of total length approximately 23 km, which has been designed to be excavated both by TBM and New Austrian Tunnelling Method (NATM). The tunnel passes under an urban area with an overburden of 10.2 to 42.8 m along the project route. Fig. 1 illustrates the general view of segmental tunnel lining constructed by TBM and geometric features of segment C, which is used for experimental tests. Type of ring is universal and composed of six segments: four rhomboidal and two trapezoidal segments (key and counter-key). The tunnel presents an internal diameter of 5.7 m, a segment thickness of 0.3 m and an average length of 3.5 m. Thus, the segment aspect ratio that is the ratio of segment length to segment thickness is about

3

98   11.8, while the tunnel aspect ratio, which is the ratio of internal diameter to ring thickness, is 19. Furthermore, two vacuum

99   holes for erector and one opening for lifting are included on the internal surface of the segments. Apart from that, totally sixteen

100   sockets (longitudinal connectors) are located on segment circumferential sides at each 22.50º for connection with the adjacent

101   rings.

102

Internal diameter: 5700 mm
External diameter: 6300 mm
Thickness: 300 mm
Average length: 3534 mm
Width: 1400 mm
Shape: Rhomboidal

103

104   (a)   (b)
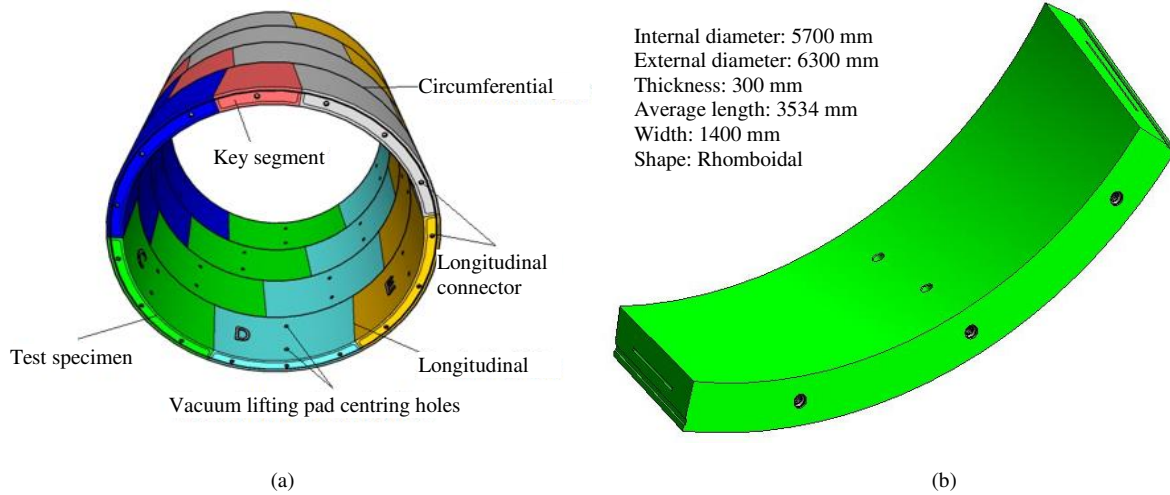
105   **Fig. 1.** Three-dimensional view of segmental lining (a) and general features of segment C (b).

106

107   In order for moving forward, TBM uses the previously placed lining ring as a reaction frame and it applies 16 loading

108   shoes to the whole ring. Based on the manufacturer's report, in exceptional cases, the maximum total ring load of the TBM is

109   40 MN, which means that the maximum thrust load that can be applied on a single pad is 2,500 kN. In the adopted configuration

110   of TBM, except for the key segments, all segments are subjected to the actions of three loading shoes, leading to a total load of

111   7,500 kN. Before thrust load being applied in the lining rings, segments are mainly subjected to transient phases in which

112   flexural and shear resistance are required (Conforti el al., 2019). The transient stage includes the demoulding, storage,

113   transportation and handling of the precast tunnel segments. In all of the transient stages, the section is subjected to bending

114   moment without axial forces. The design values of segments of the MM project for provisional phase were determined by the

115   following loading conditions:

116   -   Demoulding phase: the main load acting in the segment is due to the segment self-weight which is nearly 37 kN.

117   Based on the 1.35 load factor and 1.5 dynamic shock factor, design values for flexure and shear were calculated

118   as 31.31 kN.m and 37.57 kN, respectively (only one lifting point placed in the middle of the segment was

119   considered).

120   -   Storage phase: design values for flexure and shear were calculated as 44.25 kN.m and 128.09 kN, respectively (all

121   six segments of one ring are piled up in one stack considering an eccentricity of 0.3 m, as well as a 1.35 load factor

122   was considered);

4

123   -   Transportation phase: design values for flexure and shear were calculated as 40.08 kN.m and 104.46 kN,

124   respectively (three segments are piled up in one stack considering an eccentricity of 0.3 m, as well as 1.35 load

125   factor and 1.5 dynamic shock factor were considered);

126   -   Handing phase: design parameters are considered the same as the demoulding phase, but the compressive strength

127   of concrete is expected to reach 40 MPa.

128   Given the design values, the adopted segments must meet the minimum bending moment of 44.25 kN.m and a shear

129 action of 128.09 kN for the transient stage. Considering the difficulties of experiments on rings like Luttikholt's (2007) research,

130 only one type of full-scale precast tunnel segment (*segment C*) of MM metro project was selected for the experimental study.

131 This is because the segment C is placed at the bottom during the storage phase and is exposed to high forces compared to the

132 others during construction and transient. A total of sixteen segments with four different reinforcement solutions were produced

133 and ten of them subjected to the flexural test (2 samples for each A and D type segments, 3 samples for each B and C type

134 segments), while four (1 sample for each type) were used for the point load test. Indeed, conventional steel reinforcement is a

135 reference sample that is currently used in tunnel, while others designed as an alternative case for the similar metro tunnel

136 projects in Turkey. Although some design codes/guidelines are available for the design of fibre reinforced precast tunnel

137 segments, most of these codes are for steel fibre reinforced members. More importantly, there are limitations of

138 codes/guidelines for the design of fibre reinforced concrete tunnel segments reinforced with FRP bars (Demir, 2019). Therefore,

139 the quantity of fibres and rebars were determined based on a preliminary design of both temporary and permanent loads checks

140 for the construction of tunnel lining segments, as well as consideration of the manufacturer experiences. The adopted method

141 in the study is to compare the structural performance of possible alternative solutions. To do all this, full-scale tests are one of

142 the effective ways to investigate the mechanical and structural behaviour of fibre-reinforced concrete segments, so this study

143 followed the experimental procedure that is recommended by ITA report n.16, (2016). The analysed precast tunnel specimens

144 are:

145   A.   Typical conventional reinforcement (RC segments);

146   B.   Combination of polypropylene fibres and traditional reinforcing bars also referred to as a classical hybrid solution

147   (RC +PFRC segments);

148   C.   Combination of polypropylene fibres and glass fibre reinforced polymer reinforcing bars, innovative hybrid solution

149   (GFRP + PFRC segments);

150   D.   Polypropylene macro-synthetic fibres only (PFRC segments).

151   Fig. 2 displays the general view of the reinforcement details of test specimens. Type A consists of traditional steel

152 reinforcement which was used as reference samples. This reinforcement solution is characterized by a total steel content equal

153 to 160 kg. In other words, this can be considered as 108.3 kg/m^3. Curved rebars 8Φ10 (poses 1&3 in Fig. 3) and 4Φ12 (poses

154 2&4 in Fig. 3), which are corresponding to the longitudinal reinforcement ratio under flexure (ρ_s) of 0.32%, were located at the

155 bottom and top segment for flexure. This is higher than the minimum amount of flexural reinforcement requirement for RC

members (0.26.f_{ct}/f_{yk} = 0.21%) according to Model Code 2010. Stirrups Φ10 with 2 legs (pose 5 in Fig. 3) were used as shear

reinforcement. However, the adopted segment does not satisfy the minimum shear reinforcement ratio of Eurocode 2. In fact,

the segment shear resistance without shear reinforcement is higher than the design shear force. Moreover, local tie Φ8 with 1

leg (pose 8 in Fig. 3) were used to cope with the splitting stresses, while curved bars 4Φ12 (poses 6&7 in Fig. 3) were used for

spalling stresses.

Fig. 2. General view of reinforcement details of A, B and C type specimens.

Type B comprised of the combination of conventional steel reinforcements and PP fibres. They are characterized by

42.1 kg/ m³ typical steel and 4 kg/m³ (V_f = 0.44 %) PP fibre content. Curved rebars 4Φ12 (poses 1&2 in Fig. 4), which is

corresponding to the longitudinal reinforcement ratio under flexure (ρ_s) of 0.13%, were used for flexure and partially helping

of PP fibres for resisting spalling stresses. Stirrups Φ8 with 2 legs (pose 6 in Fig. 4) were exploited to cope with the splitting

and shear stresses. For the B4 specimens, the total number of stirrups in the curved side was preferred fifteen instead of twenty.

The polypropylene fibre reinforcement can be considered to resist splitting and shear stresses for tunnel segments, also to obtain

better control of spalling stresses (Conforti et al., 2017). Compared to the type A, the traditional steel reinforcement content of

this hybrid solution was reduced by 61% by using MSFs. This classical hybrid solution is based on a combination of fibres and

steel reinforcing bars recommended by Plizzari and Tiberti (2007). In addition to this proposal, as mentioned before

experimental programs on precast tunnel segments carried out by De la Fuente et al. (2012) and Conforti et al. (2017) represent

competitive solutions and show significant examples of hybrid cases. Particularly, Conforti et al. (2017) demonstrated that it is

possible to use smaller values of ρ_s than code requirements for conventional RC elements.

Type C consisted of both glass fibre reinforced polymer (GFRP) rebars and PP fibres. GFRP + PFRC segments were

designed as an alternative hybrid solution to eliminate the corrosion problems in tunnels. This reinforcement solution is

characterized by combination of 4 kg/m³ (V_f = 0.44 %) PP fibres content with total 28.20 m ϕ8 and 44.70 m ϕ10 GFRP rebars.

Similar to the type B, longitudinal reinforcements 4ϕ10 (poses 1&2 in Fig. 5) were used for flexure and partially helping of PP

fibres for spalling stresses. Local stirrups ϕ8 with 2 legs (pose 6 in Fig. 5) were placed for splitting stresses. Since the shear

182 capacity of GFRP bars is limited compared to conventional reinforcement, PP fibres were considered to resist shear stresses in

183 precast tunnel segment.
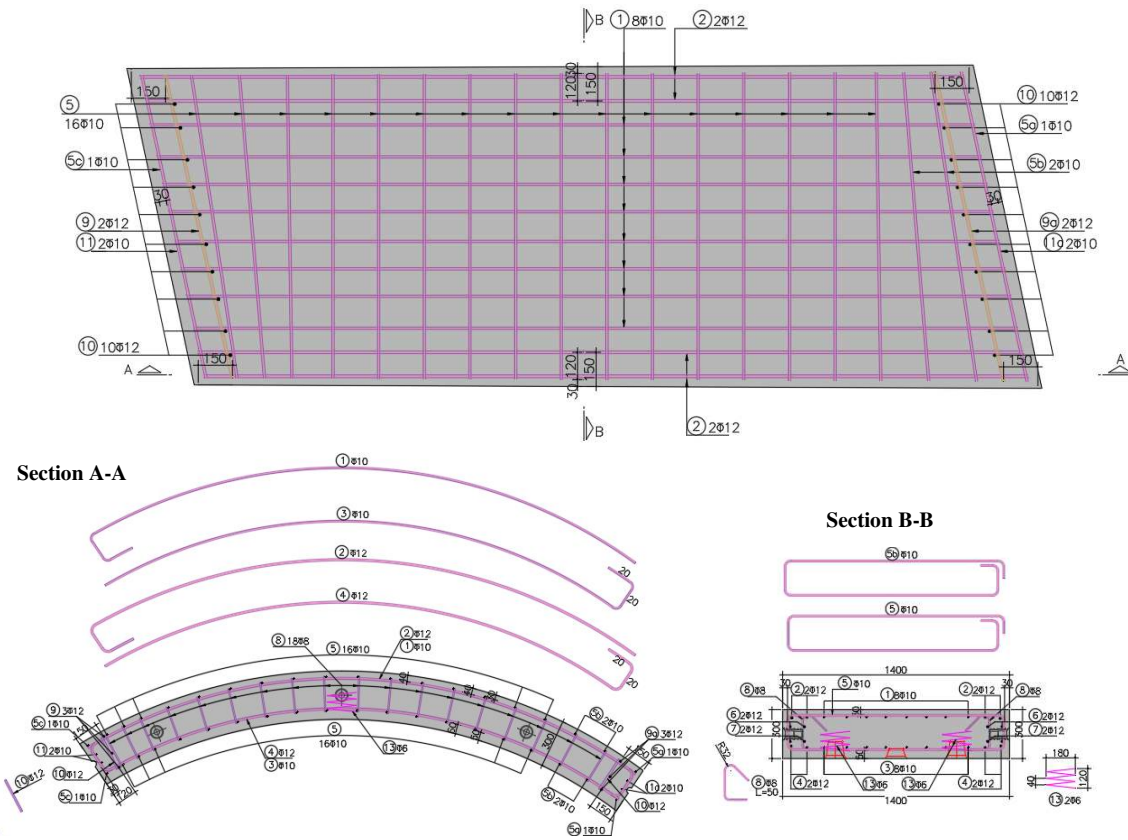
Fig. 3. Reinforcement details of RC segments (units mm, not to scale).

188   Type D was reinforced only by 6 kg/m^3 (V_f = 0.66%) polypropylene MSFs, considering a solution only by using fibres

189 for the flexural, shear, spalling, and splitting stresses. Although the amount of fibres selected is lower compared to similar

190 experimental programs (Tiberti et al., 2015; Conforti et al., 2016; Conforti et al., 2017) and ITA report n.16, (2016) suggestion,

191 which ranges from 8 to 10 kg/m^3 dosage for MSFs, it was assumed to be a guide for determining of quantity for the future

192 works. Moreover, the reason why 6 kg/m^3 MSF were chosen in the mix design is that comparison cost analysis with the RC

193 segment type was made. Since the workability of concrete is getting harder with the increasing fibre quantity, chemical

194 admixtures are needed in the concrete mix to easy the casting process. This results in increasing the total cost of the concrete,

195 considering the fibre cost, as well. The detail information about the theoretical design procedure of type C and type D specimens

196 can be found in Demir (2019).
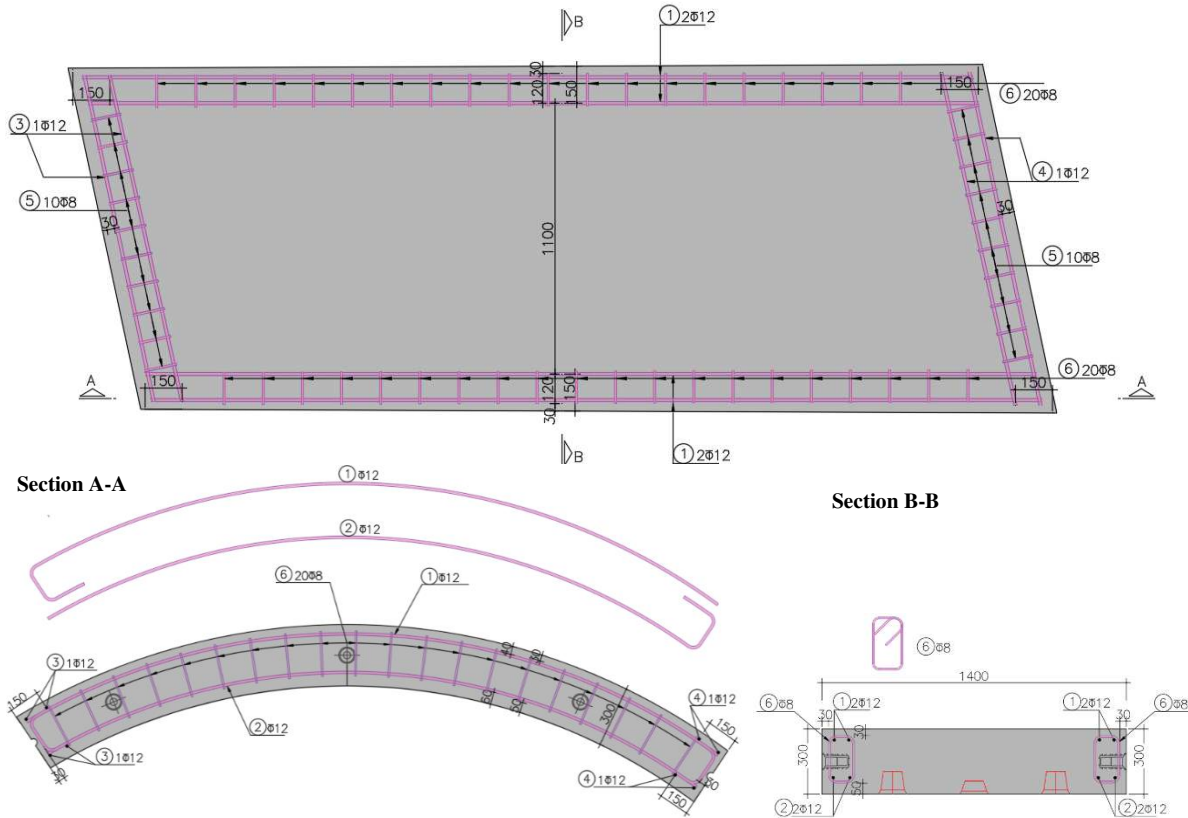
199

Section A-A

Section B-B

200

201 **Fig. 4.** Reinforcement details of RC + PFRC segments (units mm, not to scale).
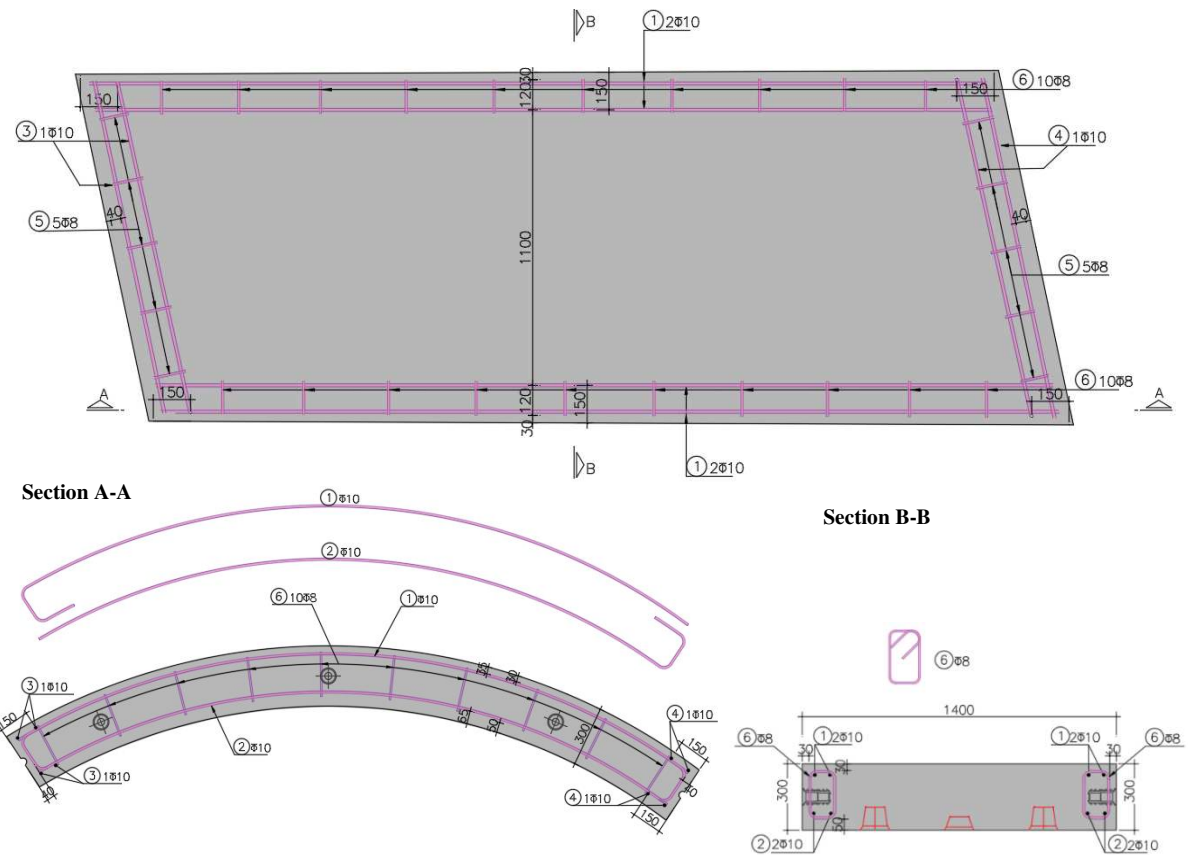
202

Section A-A

Section B-B

203

204 **Figure 5** Reinforcement details of GFRP + PFRC segments (units mm, not to scale).

205   *2.2 Materials*

206   Table 1 represents the mix proportions of concrete for the production of test specimens, namely PC and PFRC. The PC

207   mix design is used for tunnel segments with conventional reinforcement. The PFRC was used for both RC + PFRC and GFRP

208   + PFRC hybrid segments with the same amount of fibre. Moreover, the last one represents the mix design which corresponds

209   to the MSFs only. All the mix designs were provided from the ready-mixed concrete plant at the precast manufacturing yard

210   that produced four concrete batches. In this experimental program, the C40/50 concrete class was chosen to produce specimens

211   according to EN 1992-1.1 (2004). With reference to this code, the target average cylindrical compressive strength, which is

212   generally adopted in practice at 28 days, is about 48 MPa (f_{cm} = f_{ck}+ 8 MPa). The specimens were cast in steel moulds and

213   consolidated with the help of a vibration system. All concrete mixes displayed sufficient workability without considerable

214   reduction of their flowability from the beginning to the end of the casting process. Furthermore, all specimens were cured in

215   the steam-curing chamber approximately 5.5 hours before demoulding to obtain concrete with a minimum compressive strength

216   of f_{ck} = 15 MPa. Then all specimens stored at the precast manufacturing yard up to testing (age of 28–90 days). Table 2

217   summarizes the PP macro-synthetic fibre characteristics based on the EN 14889-2 (2006).

218

219   **Table 1** Concrete mix design of specimens.

Sample type	A	B & C	D
Concrete designation	PC	PFRC	PFRC
Cement type	CEM I	CEM I	CEM I
Cement content (kg/m^3)	365	374	385
Water (L/m^3)	152	142	146
W/C Ratio	0.42	0.38	0.38
Admixture (kg/m^3)	3.33	3.23	3.71
Crushed sand (kg/m^3)	361	361	358
Aggregate 5-12 (kg/m^3)	498	498	494
Aggregate 12-19 (kg/m^3)	413	395	392
Aggregate 19-25 (kg/m^3)	585	604	599
Fibre content (kg/m^3)	-	4	6
Fibres V_f(%)	-	0.44	0.66

220

221   **Table 2** Polypropylene macro-synthetic fibre properties.

Type:	Polypropylene
Length (mm):	54
Diameter ϕ (mm):	0.677
Aspect ratio $1/\phi$:	79.76
Tensile strength (MPa):	550-750
Elastic modulus (MPa)	5750
Density (kg/m^3)	910
Number of fibres per kg (approximately)	220000

222

223   In all four concrete batches, six cubes (150 mm side dimensions) were cast to determine the compressive strength at

224   ninety days, while three cylindrical samples (100 x 200 mm) were prepared to measure the compressive strength at both seven

225   and twenty-eight days according to EN 12390-3 (2009). Besides, nine small beams (150 x 150 x 550 mm), three samples for

226   each mix designs which consist of MSFs, were prepared to evaluate the fibre reinforced concrete (FRC) residual flexural tensile

227   strengths according to EN 14651 (2005).

9

228   Based on EN 14651, nominal stress versus crack mouth opening displacements (CMOD) curves from three small beams

229   of each FRC sample are displayed in Fig. 6. Experimental result of bending test demonstrated that all FRC samples show

230   flexural softening behaviour since there was no considerable increase in stresses after the first crack (see Fig. 6). Apart from

231   that, multiple cracking was not observed on any of the FRC samples.

232
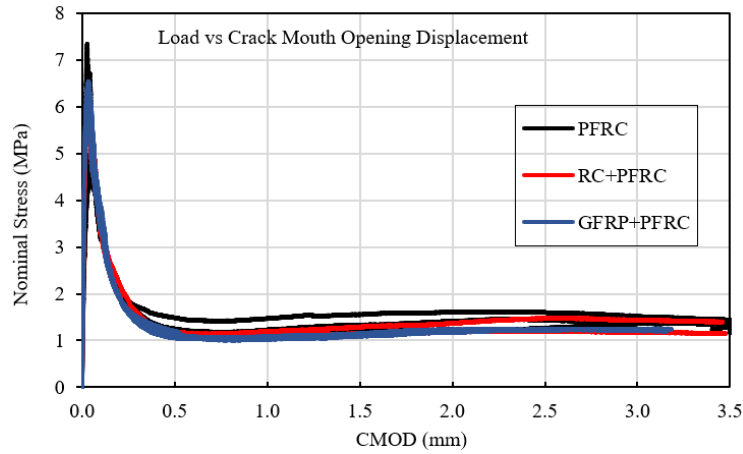
233

234   **Fig. 6.** Load versus crack mouth opening displacement (CMOD).

235   Table 3 summarizes the mean mechanical properties of the four concrete batches that were evaluated cubes (at 90 days)

236   and cylinders at both 7 days and 28 days. Coefficient of variances (CVs) is also provided in brackets. The mean cylindrical

237   compressive strength (f_{cm}) result of all samples provided target values of 48 MPa, it varies from 48.3 to 55.2 MPa.

238

239   **Table 3** Residual tensile strengths of test specimens and compressive strength of concrete.

Specimen	RC	RC+PFRC	GFPR+PFRC	PFRC
$f_{cm,cube}$ (MPa)	62.57 (0.05)	60.15 (0.03)	64.09 (0.01)	68.96 (0.02)
$f_{cm,cylinder}$ (MPa)	49.90 (0.04)	48.30 (0.03)	50.10 (0.01)	55.20 (0.01)
$f_{cm,cylinder,\ 7\ days}$ (MPa)	41.30 (0.01)	41.50 (0.01)	42.30 (0.01)	47.70 (0.01)
$f_{L,m}$ (MPa)	-	6.08 (0.04)	6.46 (0.02)	5.64 (0.27)
$f_{R,1m}$ (MPa)	-	1.16 (0.03)	1.13 (0.06)	1.32 (0.12)
$f_{R,2m}$ (MPa)	-	1.19 (0.07)	1.13 (0.02)	1.37 (0.13)
$f_{R,3m}$ (MPa)	-	1.30 (0.12)	1.23 (0.01)	1.44 (0.12)
$f_{R,4m}$ (MPa)	-	1.26 (0.14)	-	1.36 (0.06)

240

241   The limit of proportionality f_L and the residual flexure tensile strengths (f_{R1}, f_{R2}, f_{R3}, f_{R4}, corresponding to Crack Mount

242   Opening Displacements values of 0.5, 1.5, 2.5 and 3.5 mm, respectively) and CVs are stated in Table 3. According to ITAtech

243   report n.7 (2016), typical minimum performance levels for tunnel segmental linings under the bending effect should be f_{R1k} >

244   2.2 MPa and f_{R3k} > 1.8 MPa in terms of residual tensile strength after the 28 days. However, it is observed that 6 kg/m^3 PP

245   fibres have not provided significant structural performances both at SLS (f_{R3m} of about 1.44 MPa) and ultimate limit states

246   (ULS) (f_{R1m} of about 1.32 MPa) since the results are considerably lower than expected. Similarly, samples that contain 4 kg/m^3

247   fibres displayed low residual flexural tensile strength. Based on the results, the RC + PFRC and PFRC samples were classified

248   as 1c, while the classification of GFRP + PFRC sample was found 1d according to Model Code 2010.

10

249   Fibre reinforcement can substitute (even partially) the conventional reinforcing bars or steel mesh at the ULS, if both

250   the relationships (f_{R1k}/f_{Lk} >0.4 and f_{R3k}/f_{R1k} >0.5) are fulfilled according to fib Model Code 2010, (2012). Based on the

251   experimental results, the following ratios were obtained: f_{R1k}/f_{Lk} = 0.2 and f_{R3k}/f_{R1k} = 1.02 for RC+ PFRC; f_{R1k}/f_{Lk} = 0.17 and

252   f_{R3k}/f_{R1k} = 1.15 for GFRP+ PFRC; f_{R1k}/f_{Lk} = 0.28 and f_{R3k}/f_{R1k} = 1.1 for PFRC. Thus, samples do not fulfil the requirements of

253   the Model Code 2010 criteria for use in structural elements considered the ULS. Moreover, PRFC samples did not satisfy the

254   criteria that the minimum amount of conventional shear reinforcement is not needed if the characteristic value of ultimate

255   tensile strength (considering with w_u=1.5 mm) for fibre reinforced concrete is higher than the limit ($f_{Ftuk} \geq 0.08\sqrt{f_{ck}}$) according

256   to equation 7.7-14 of MC 2010. Characteristic values were obtained by considering the equation that is given in the ITAtech

257   report n.7 (2016); $f_{fctk} = f_{fctm}$ x (1-0.95 *V_x). In summary, although this study focuses on allowable SLS for tunnel segments,

258   results of EN 14651 test indicated that the adopted fibre amounts are not suitable for significant post-cracking residual strengths.

259   Preferred concrete matrix did not meet the criteria of Model Code 2010 for both structural applications and using only PP fibres

260   as minimum shear reinforcement.

261

262   **Table 4** Glass fibre reinforced polymer rebars properties.

Diameter Φ (mm)	8	10
Nominal cross-sectional area (mm^2)	50	80
Elastic modulus (GPa)	50.2	51.7
Ultimate strength (MPa)	997	895
Coefficient of thermal expansion (Longitudinal direction, 1/°C)	2.2×10^{-7}	2.2×10^{-7}
Rupture strain (%)	4.50	6.40
Shear strength (Transverse direct., MPa)	222	248

263
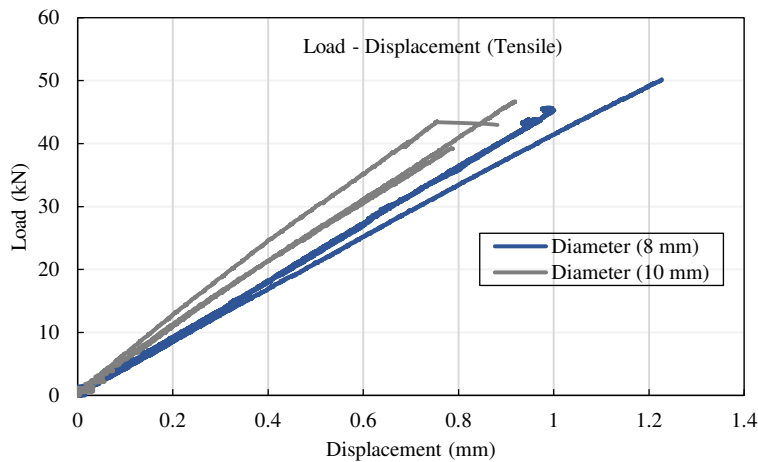
264

265   **Fig. 7.** Load versus displacement curve of GFRP rebars.

266

267   Table 4 summarizes the GFRP rebar characteristics which were taken from the related company's catalogue prepared

268   according to ISO 10406-1 (2008). In addition, experimental set up was prepared to measure ultimate tensile capacity for GFRP

269   rebars in accordance with ASTM D7205 standard. Tensile tests were performed for both Φ8 and Φ10 reinforcements in the

270   samples which are taken from the field. In this experiment, 9 specimens for Φ8 and 8 specimens for Φ10 were tested but

11

271 displacement values were recorded for 3 specimens of each reinforcement (Fig. 7). As expected, GFRP rebars showed linear

272 behaviour until failure. The ultimate tensile strength of the $\Phi 8$ reinforcement, which has a 50 mm^2 nominal cross-sectional

273 area, was calculated to be 904 MPa. This value is very close to the ultimate strength (895MPa) that is used in the preliminary

274 design. However, for $\Phi 10$ rebars, which have 78.5 mm^2 nominal cross-sectional area, the average value was measured as 600

275 MPa. This finding is 39% less than the expected strength capacity of 977 MPa (Table 4). Moreover, the experimental curve

276 displayed that there are significant differences in stiffness of the tested bars (Fig. 7). This suggests that the flexural capacity of

277 type C segments will be lower than expected due to low production quality.

278 Considering conventional steel reinforcing bars, three different steel deformed reinforcements with diameters ($\Phi 8$, $\Phi 10$

279 and $\Phi 12$) were used as both transverse and longitudinal reinforcement in the production of precast tunnel segments. However,

280 since the rebars properties did not measure by means of experimental way, S420 class steel reinforcement properties have been

281 considered by TS-708-2010 specification. According to related specification, minimum yielding and ultimate tensile strength

282 of these steel reinforcement should be 420 MPa and 500 MPa, respectively and it is assumed that they satisfy the minimum

283 criteria of the specification.

284 **3. Flexural test**

285 The full-scale flexural tests are useful tools to provide the design approach (ACI Committee 544, 2016; ITA report n.

286 16., 2016). For the current research, the main purpose of the flexural test is to measure and compare the flexural bearing capacity

287 of specimens at the allowable SLS. Since segments are subjected to flexure during demoulding, transportation and storage, the

288 aim of the flexure test is to analyse whether the segments meet the criteria during these phases. Design moment for the

289 production and transient phase of MM metro project is approximately 44.25 kN.m. This was calculated by the scenario that

290 each ring can be stacked in one pile at storage phase and the distance between two bearing timbers was taken 2.3 m with an

291 accidental eccentricity (e = 0.30m) concerning the supports. In this experiment, crack width opening due to flexure and mid-

292 span deflections of the segment were measured to evaluate the specimen's capacities. To determine the maximum bending

293 moment capacity of specimens, allowable SLS crack width was taken into consideration. In this experimental program, the

294 crack width limit was considered to 0.3 mm, which is based on the MM project criteria.

295 *3.1 Experimental set-up of the flexural test*

296 In accordance with the previous experimental tests (Caratelli et al., 2012; Abbas et al., 2014b; Meda et al., 2016;

297 Conforti et al., 2017), three-point bending test was adopted to evaluate the flexural behaviour of full-scale precast tunnel

298 segments (Fig.8). In this test, the load was applied to the segments to the outer face by two loading steel plates (200x200 mm)

299 on the mid-span. In addition, the rubber layer having a 20 mm thickness, Teflon, and another 10 mm rubber layers were placed

300 at the bottom of steel plates to obtain full contact with the surface. The above-mentioned load was applied to the system by

301 means of a hydraulic jack with a loading capacity of 500 kN and applied load levels were measured by load cell during

302 experiments. However, the load has not been applied with a displacement-controlled hydraulic jack, therefore, it was paid

303 attention to applying load rate as close as possible during experiments. Apart from that, two roller supports were placed

304 continuously on the entire segment width, providing that 2.6 m net span length between these supports.

305
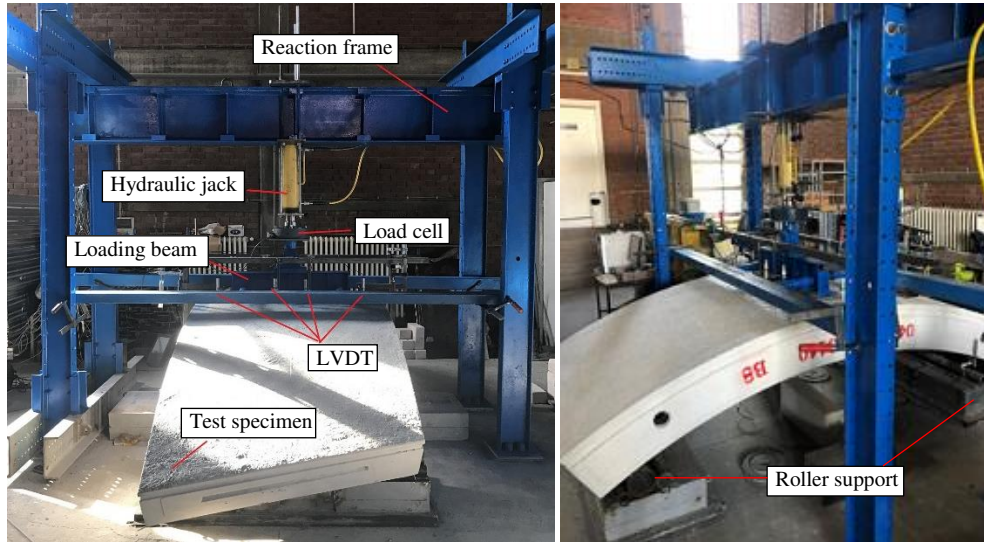
306

307 **Fig. 8.** Loading systems of flexural test (a) and frontal view of test set-up (b).

308

309   Linear Variable Differential Transformers (LVDTs) were installed to the specimens to measure flexural crack opening

310 width and mid-span deflections. Two LVDTs (CWL and CWR) were placed on the segment's inner surface to measure the

311 crack opening width due to flexure. Similarly, two strain gauges (SG1 and SG2) were also placed on the segment's inner

312 surface to evaluate the first cracking load level. Since the maximum flexural moment occurs at the mid-span of the specimen

313 due to three-point bending test system and the weakest section of the segments is in the middle zone because of the holes,

314 measuring devices were installed to this region. 6 LVDTs were placed outer surface of specimens to evaluate the mid-span

315 deflection of segments. Deflections were measured by identifying vertical displacement of segments during the test. The

316 average value was obtained from the four LVDTs which were in the middle (D3, D4, D5, and D6), while the others measured

317 left and right sides deflections of the mid-span (D1 & D2). In addition, horizontal displacements were measured by means of

318 two LVTDs which are located at two longer corners of segments (H1 and H2). The instrumentations details and general view

319 of the flexural test are shown in Fig. 9.

320

321

322

323

324

13
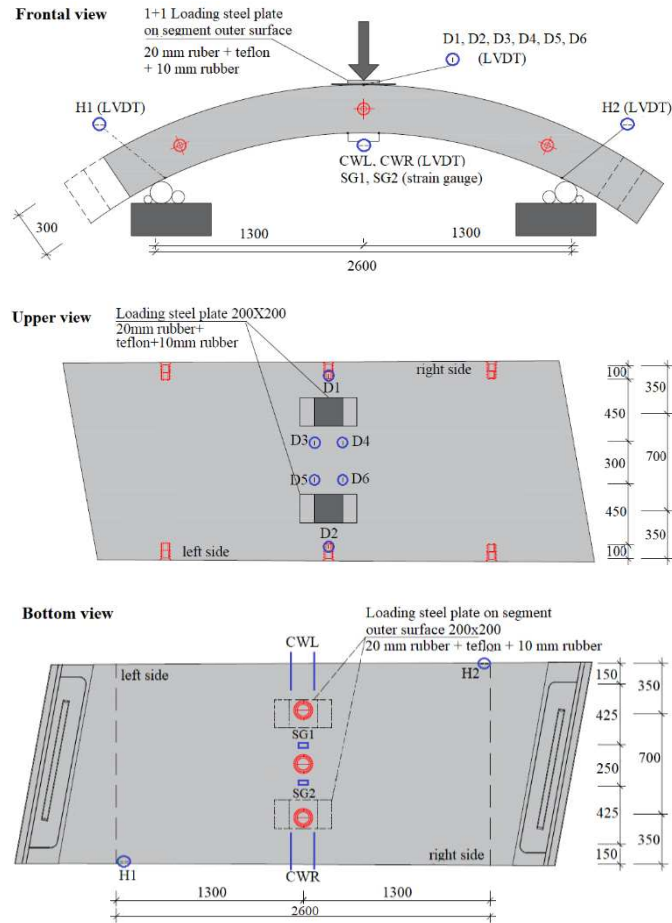
Fig. 9. Instrumentation details of the flexural test (units mm).

3.2 Experimental results of flexural test

Table 5 summarises the load levels at the first crack observation on specimens ($P_{cracking}$) and corresponding moment ($M_{cracking}$) and deflection ($\delta_{cracking}$) at $P_{cracking}$. The table also shows the load levels at the allowable crack width (0.3mm) limit (P_{SLS}) and corresponding moment (M_{SLS}) and deflection (δ_{SLS}) at P_{SLS}. The experimental curves of load versus flexural crack opening width are displayed in Fig. 10. In addition, Fig. 11 shows the load versus mid-span deflection of segments. The first cracking of RC specimens (A1 and A2) occurred at a load of about 77 and 86 kN, respectively. Corresponding moment values of these loads were nearly 59 and 64 kN.m. In the flexural test, moment on the segments was calculated by following the equation (M = 8.63 kN.m + 0.65xP kN.m). The constant part in the equation represents the moment caused by self-weight of the specimens, while the second part is the effect of the applied load. Given this formula, the load corresponding to the design moment of 44.25 kN.m is found as approximately 55 kN. When the opening crack width reached the SLS limit, the load (P_{SLS}) was measured as about 145 kN for both RC specimens. This indicates that measured moments at SLS crack limit are 1.75 and 1.59 ($M_{SLS}/M_{cracking}$) times higher than their first cracking moments, respectively (see Table 5). It should be noted that $M_{cracking}$ of RC specimens resulted in about 40% greater than the design bending moment (44.25 kN.m), which is important because flexural cracking of segments should be avoided at any phase of the project (Conforti et al., 2017).

14

343   Contrary to adopted structural ductility term in the technical literature, since this research focuses on the SLS limit

344   rather than ULS, to make a comparison between specimens, the deflection ratio was calculated as the ratio of deflection of at

345   the SLS crack width limit to the at the value at the first visible flexural cracks. Given the results in Table 5, the deflection ratio

346   of A1 and A2 specimens ($\delta_{SLS}/\delta_{cracking}$) was calculated as approximately 3.7 and 3.4, respectively. Considering the final situation

347   of the tunnel, these experimental results indicate that RC segments have stable post-cracking response under flexure, which is

348   important for workers since this enables them to escape in case of exceptional events (ITA Report n.16, 2016). Although

349   applying the load until the failure of the samples is important for evaluating the failure mode and determining the ultimate

350   bearing capacity, the load level applied after the SLS crack limit has not been increased for safety reasons. Because the main

351   purpose of the flexural test in the present study is evaluating the flexural behaviour of specimens at the SLS limit.

352

353   **Table 5** Load and corresponding moments and deflections.

Specimen	RC		RC + PFRC			GFRP + PFRC			PFRC	
	A1	A2	B2	B3	B4	C2	C3	C4	D1	D4
First crack										
$P_{cracking}$ (kN)	77.3	85.8	69.9	-	68.5	-	69.4	-	59.4	89.4
$M_{cracking}$ (kN.m)	58.9	64.4	54.1	-	53.2	-	53.7	-	47.3	66.7
$\delta_{cracking}$ (mm)	0.80	0.93	0.74	-	0.70	-	1.05	-	0.86	0.98
SLS crack limit - 0.3 mm										
P_{SLS} (kN)	145.3	143.9	119.4	93.8	91.8	70.4	68.2	79.2	64.7	78.7
M_{SLS} (kN.m)	103.1	102.2	86.2	69.6	68.3	54.4	53.0	60.1	50.7	59.8
δ_{SLS} (mm)	2.96	3.18	2.45	2.08	1.86	1.47	1.70	1.74	1.66	1.53

354

(a)   (b)
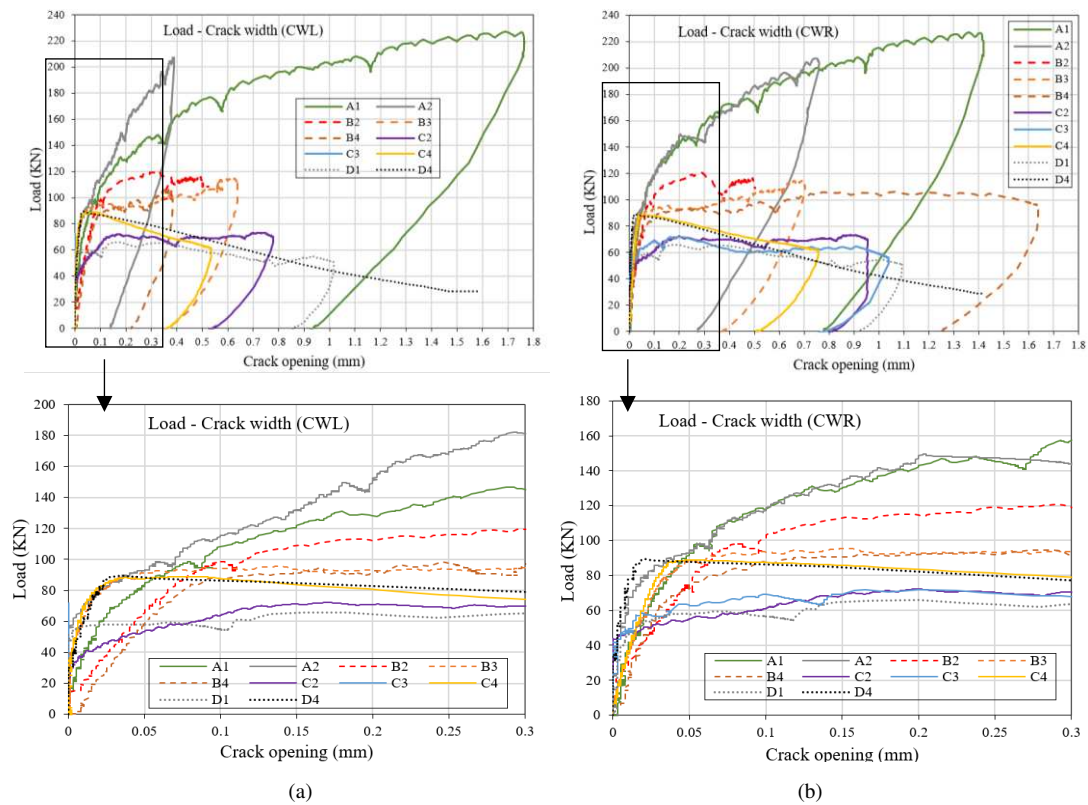
355   **Fig. 10.** Load versus flexural crack width (a) obtained by CWL (b) obtained by CWR.
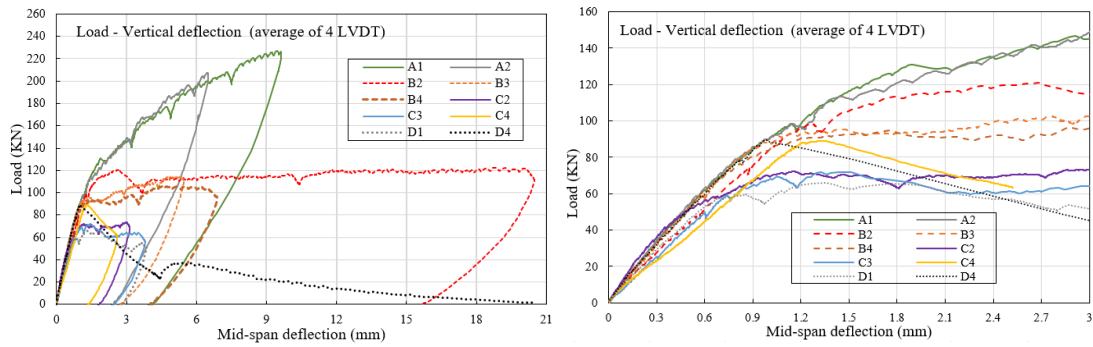
Fig. 11. Load versus mid-span deflection curve (average of D3, D4, D5, and D6),

RC + PFRC hybrid segments, which are the combination of PP fibres and conventional steel reinforcements, also showed sufficient structural performance under the flexure for MM project. The measured moment at both the first structural cracking occurred and at the allowable SLS crack limit satisfies the design criteria of production and transient stages. The first structural cracking of RC + PFRC specimens (B2 and B4) occurred at about 70 and 69 kN load levels, respective1y. At the flexural opening width of specimens (B2, B3 and B4) reached the allowable crack limit, the loads were recorded as 119.4, 93.8 and 91.8 kN respectively. This indicates the moment of RC segments at SLS (M_{SLS}) are 1.6 and 1.3 times higher than their first cracking moments ($M_{cracking}$) for B2 and B4 samples, respectively. It should be noted that the number of stirrups in the segment affects the bending capacity after cracking occurs. Therefore, the experimental bending capacity of the B4 sample was observed to be lower than other RC + PFRC segments due to its fewer stirrups. The positive effect of macro-synthetic fibres was observed in RC + PFRC segments, especially in terms of energy absorption capacity (Fig. 11). RC + PFRC segments have also significant deflection ratio ($\delta_{SLS}/\delta_{cracking}$) and it is nearly 3.31 and 2.66 (due to fewer stirrups) for B2 and B4 specimens, respectively. Although a longitudinal reinforcement ratio was 40.6% smaller than RC ones, the deflection ratio of B2 specimen is very close to RC segments. Considering the post-cracking stiffness of RC + PFRC segments, it showed high resistance up to a certain crack width. However, after cracking width reached the serviceability limit the resistance level decreased (always remaining greater than cracking load) up to unloading time. In fact, RC + PFRC segments exhibited a hardening behaviour under flexure after first cracking of concrete occurred, with multiple cracking was observed on segments (Fig. 12).

Considered to another hybrid solution (GFPR + PFRC), even though the flexural capacity of segments at the initial crack occurrence satisfied the design criteria, they did not show stiffer behaviour under the flexure compared to RC+PFRC specimens. The behaviour of GFRP + PFRC segments was remarkably different from segments contains traditional reinforcement. $P_{cracking}$ of C3 specimen was detected at 69 kN. Thereafter, the stiffness increased slightly up to 72 kN because of the stress transmitting along the cracks providing by fibre reinforcement. At this stage, the specimen has reached the maximum bearing capacity that was calculated nearly 55 kN.m and with 0.2 mm crack width. Afterwards, a softening branch was developed, and the resistance started dropping in a stable way and the critical crack continued to open. When the critical crack width reached the serviceability limit, 53 kN.m bending moment was measured on the segment. Similarly, during the

16

383   experiment of C4 specimen, the same structural behaviour was observed, but the C2 specimen had more post-cracking stiffness

384   compared to C3. It reached the maximum load level that is nearly 73 kN after the serviceability crack limit. The crack with

385   corresponding to maximum load is about 0.71 mm and this is approximately 2.4 times higher than serviceability limit. The

386   deflection ratio ($\delta_{SLS}/\delta_{cracking}$) for C3 specimen is about 1.62. However, it should be noted that opening the flexural crack width

387   at the left side of the C3 could not be measured because the crack occurred in the area where width measurement is not possible

388   by CWL (Fig 10a).

389   As far as the PFRC segments are concerned, it was observed that a similar scenario observed with the GFRP + PFRC

390   specimens. PFRC segments exhibited a softening behaviour under flexure due to the low quantity of PP fibres in the concrete

391   mixture. PP fibres led to a partial enhance in post-cracking stiffness after initial structural cracking. The first cracking of PFRC

392   specimens (D1 and D4) occurred at about 59 and 89 kN load levels, respectively. After this stage, the specimens reached

393   maximum load levels at a crack width very close to the initial structural cracking values. Based on the experiment results,

394   although the bending capacity of PFRC segments fulfils the minimum requirement of design moment, the post-cracking

395   stiffness of the specimens was not at desirable level. Besides, it was seen that the ratio between maximum loads (P_{max}) and the

396   loads at which the first crack is formed ($P_{cracking}$), is very close to each other and resulted in 1.12 and 1.04 respectively. For the

397   D4 specimen, maximum load was recorded before the cracking opening reaches the SLS limit, then critical crack continued to

398   open, and the segment collapsed. Deflection of the specimens at the SLS crack limit are nearly 1.93 and 1.56 times higher than

399   initial crack observed ($\delta_{SLS}/\delta_{cracking}$). These are significantly lower compared to RC and RC + PFRC segments. In addition, the

400   test results demonstrated that PFRC segments have lower energy absorption capacity than other specimens (Fig. 11).

401   For all the segment types mid-span deflection is lower than 1 mm at the 55 kN load level that constitutes design moment

402   of the metro project. On the contrary, deflection values changed significantly between the specimens depending on the

403   reinforcement type at the high load level. It can be clearly seen that RC and RC + PFRC segments are stiffer than others.

404   Compared to load level at 3 mm deflection, RC segments are nearly twice as much stiff as than PFRC and GFPR + PFRC.

405   Moreover, when energy absorption capacities of specimens up to 3 mm deflections are considered, segments with steel

406   reinforcement shows higher capacity than other types (Fig 11).

407   Fig. 12 shows final crack patterns which observed on the inner surface of precast tunnel segments due to flexure. It can

408   be seen that the multiple cracking has occurred on RC and RC + PFRC segments. It can be noted that multiple cracking occurred

409   at the specimens that showed hardening behaviour under the flexure, on the contrary, single critical cracks occurred at the

410   segments that exhibit a softening behaviour (GFRP+PFRC and PFRC segments). Furthermore, as it is seen in the figure, almost

411   at all specimens, cracking pattern pass through the critical section that is the weakest region of the segment due to existing of

412   vacuum and longitudinal connecters holes.

17

413
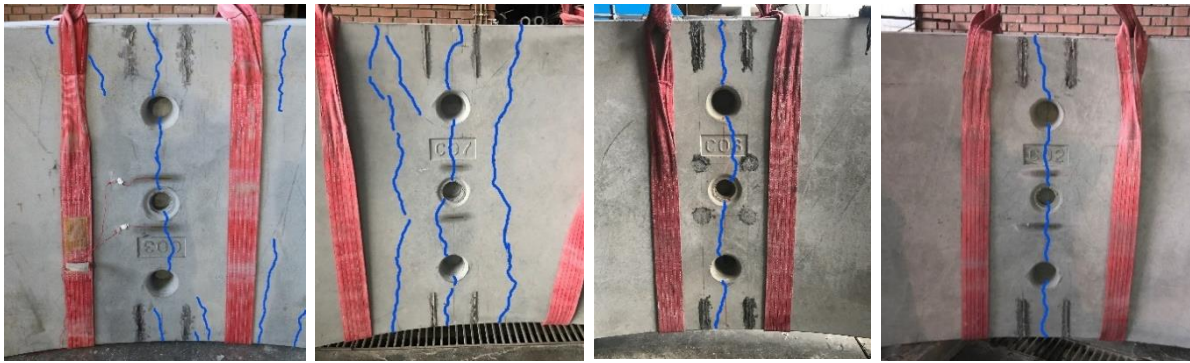
414   RC – (A2)   RC + PRFRC – (B2)   GFRC + PFRC – (C2)   PFRC – (D1)

415 **Fig. 12.** Final crack pattern of specimens (inner surface view).

416 **4. Point load test**

417   The main purpose of this test is to evaluate the structural performance of precast tunnel segments subjected to the TBM

418 actions during the excavation process of the tunnel. TBM is pushed itself forward by thrust jacks which are acting on the last-

419 placed lining ring. Even though the applying forces on the tunnel lining, which is induced by TBM thrust, is a temporary

420 loading condition for construction stages, this causes serious stresses on precast tunnel segments. Therefore, it must be properly

421 considered since this may be the most critical condition for the segment design (Meda et al., 2016). For that reason, point load

422 tests were conducted to the designed segments. The application of the high concentrated TBM thrust load on relatively small

423 surfaces causes splitting stresses or bursting stresses on a plane perpendicular to the direction of the applied thrust. Another

424 type is known as spalling stresses that they occur in the unloaded zone between the TBM rams in the circumferential direction.

425 Similar to the flexural test, allowable SLS cracking width was considered in point load test to evaluate the structural

426 performance of specimens. In addition, vertical displacements of segments and the cracking pattern was also considered.

427 *4.1 Experimental set-up of point load test*

428   In the MM metro project, an earth pressure balanced (EPB) type of TBM has been used for the construction of the

429 tunnel. Therefore, in this experiment, loading systems were adapted to reflect the actual TBM thrust loading to evaluate the

430 structural performance of precast tunnel segments. To perform a full-scale test, a suitable testing system has been designed and

431 constructed considering both actual pad configuration on segment C and geometry used by the chosen TBM (Fig. 13). Within

432 this framework, a rigid steel system, which close ring frame made with HEB 300 steel beams and 52 mm diameter stem bars

433 were designed for equal load distribution of 3 pads. In this experiment, irregularities that can occur during the segment

434 placement in the ring were not considered. Therefore, tunnel segments were placed on a stiff steel base (S235JR class and

435 dimensions 4500 x 1000 x 100 mm) that having continuous support. In the adopted configuration of TBM, maximum 2,500

436 kN load can be applied on a single pad in exceptional cases. Since three pads are placed on segment C, the maximum total load

437 capacity was considered as 7,500 kN. Based on this information, six hydraulic jacks that having a load capacity of 1,500 kN

438 each were inserted in the closing rigid ring frame. In the experimental set-up, these hydraulic jacks were located between steel

18

pads and frame and two hydraulic jacks were acted on each steel pad, which is the same dimensions as the real one. The locations of pads on the segment surface and dimensions of pads are demonstrated in Fig. 14. Applied load levels on the specimens were measured by means of pressure transducers that were located at each hydraulic jack and at the output of the hydraulic pump. All the data were continuously recorded by an acquiring digital system and transmitted to a computer during experiments.

(a)   (b)
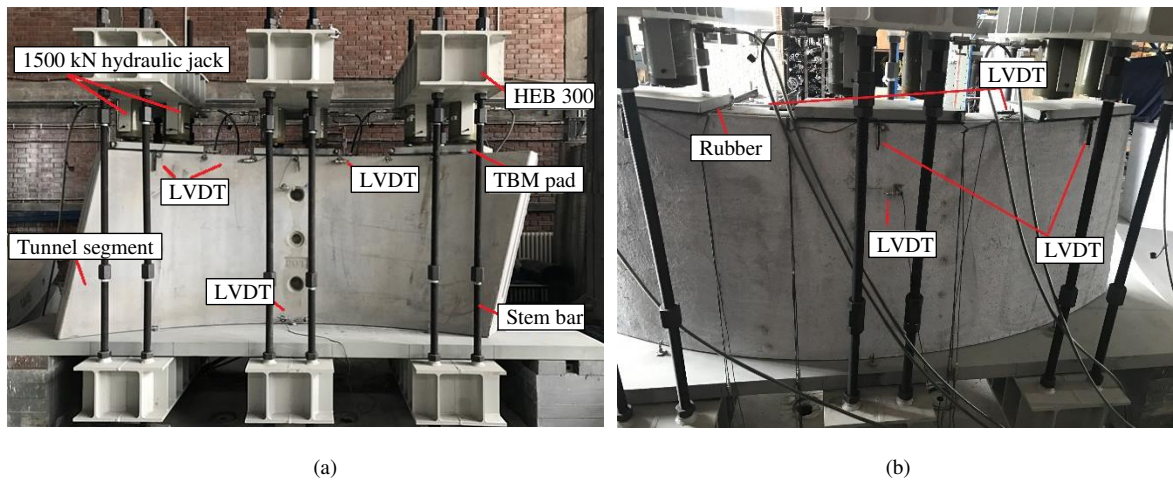
Fig. 13. Loading systems of point load test, inner surface (a) and outer surface (b).

To measure cracking width due to local tensile stresses that caused by high compression load, LVDTs were placed on the specimen surfaces. Two LVDTs (H1-T, H2-T) were located on the top sides of the segment between loading pads to record the spalling crack width (Fig. 14). Similarly, two more LVDTs (H1-I, H2-I) were located on the inner surface of the segment between loading pads. One LVDT (H3-I) was also placed under the middle loading pad near the vacuum hole to measure splitting crack width. Moreover, totally six LVTDs were placed on both outer (V1-O, V2-O, V3-O) and inner (V1-I, V2-I, V3-I) surface of segments to measure the vertical shortening of specimens under the loading plates. The locations of instruments on segments and details of the full-scale point load test are shown in Fig. 14.
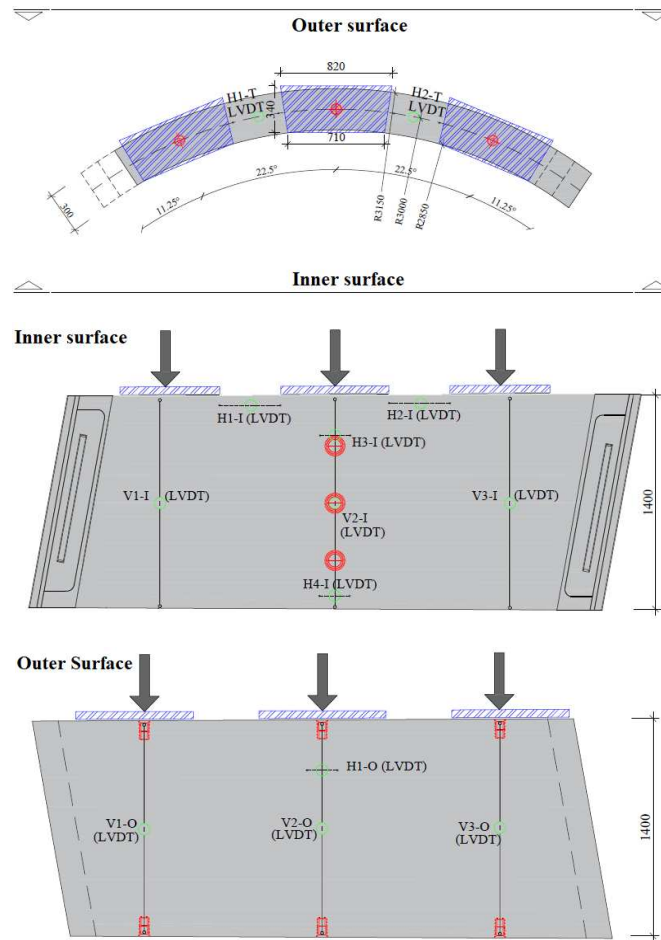
461

462

463

464 **Fig. 14.** Instrumentation details of point load test (units mm).

465 *4.2 Experimental results of point load test*

466   Fig.15 shows applied total thrust load level versus spalling cracking opening values that were obtained from H1-I (Fig.

467 15a) and H1-T (Fig. 15b). The findings in the graphs reveal that all specimens showed sufficient structural performance under

468 the maximum thrust forces level of TBM (7,500 kN) in terms of the allowable crack limit (0.3 mm). Even though measured

469 crack width from LVDTs at the top and inner surface are slight differences between, all crack formed on the specimens are

470 smaller than 0.3 mm limit. This can be caused by the location of LVDTs or the geometry of specimens. According to Fig. 15b,

471 the first crack on the top surface of all segments has occurred almost at the same load level except for GFRP + PFRC (C1)

472 segment. The first crack occurred at a higher load level than others. While the inner surface is considered, the load levels of

473 single pad corresponding to occurred first cracking for RC (A4) and RC + PFRC (B1) segments ware nearly 1700 kN and 1830

474 kN, respectively. Nonetheless, the values for both PFRC (D2) and GFRP + PFRC were considerably lower. Moreover, observed

475 cracks on the inner surface of the test specimens were marked and measured their corresponding depths. The final crack patterns

476 are shown in Figure 16.

477   However, it should be noted that the PFRC segment has a lower resistance to spalling stresses compared to other types

478 of segments. Based on the experimental results, the maximum spalling crack width was recorded as approximately 0.22 mm

20

479 on the PFRC segment's top surface (Fig. 15). The reason for that there is no reinforcement rebar in the corresponding regions
480 where the local stresses are high. Also, it may be caused by the low amount of fibre content present in the PFRC segments (V_f
481 = 0.66 %). First cracks on segments have occurred between the loading pads. Thereafter, with the increasing load, cracking
482 depth has extended along the segment width. Maximum spalling cracking depth was measured 371 mm under the 8300 kN
483 load (Fig. 16).

484
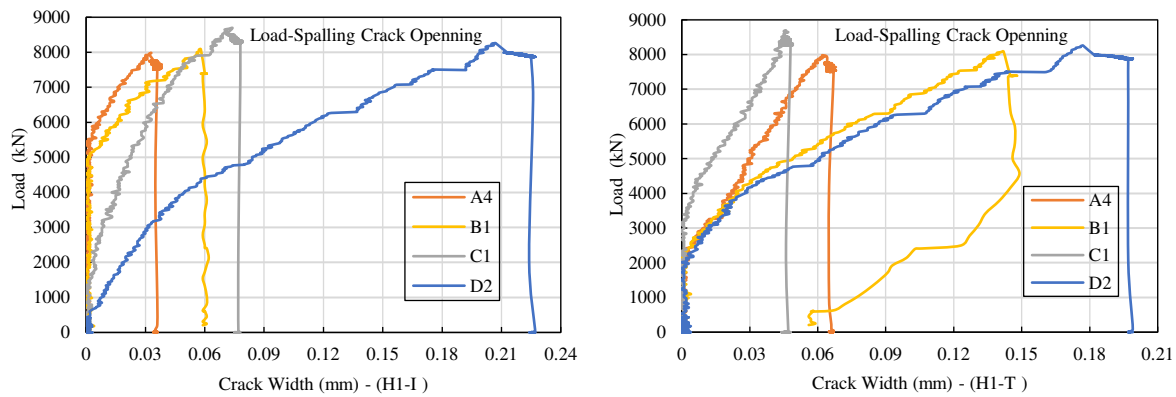
486 **Fig. 15.** Load versus spalling cracking opening width on inner surface (a) and on the top (b).

487

488   RC segment, which is the reference sample, displayed significant resistance to the thrust action. Compared to others,
489 cracking caused by splitting or bursting stresses were also observed in the RC segment (Fig. 16a). However, although more
490 cracks were observed on the segment surface, recorded cracking widths are quite smaller than others. This is because a high
491 amount of steel rebars in the segment led to the preventing of occurring larger cracks. Based on the results, maximum spalling
492 crack width was recorded as about 0.06 mm on the segment's top surface and corresponding crack depth was measured as
493 213mm, while maximum splitting cracking depth was measured as 230 mm. Apart from that, contrary to expectation, another
494 crack has emerged on the mid-region that near the base level of the test system (Fig. 16).

495   When the RC+ PFRC segment is concerned, it can be observed that the classical hybrid solution has displayed sufficient
496 structural performance against to maximum thrust effect of adopted TBM. Compared to the PFRC segment, both the cracking
497 width and depth values are significantly smaller. Based on the recorded data, maximum spalling crack width was detected on
498 the segment's top surface approximately 0.14 mm (Fig. 15b), and maximum crack depth was measured as 140 mm (Fig. 16).
499 Similar to PFRC specimen, any cracks caused by splitting or bursting stresses were not observed on the segment.

500   Considered the innovative hybrid solution, which is comprised of the combination of glass fibre reinforced polymer
501 (GFRP) rebars and PP fibers, showed also well sufficient performance under the applied maximum thrust forces. Maximum
502 spalling crack width was recorded by LVTDs on the segment's inner surface approximately 0.08 mm. However, there was no
503 crack observed on the specimen surface, although, applied load level pretty much higher than the others. This may be due to
504 the presence of GPRP in the segment which provides a higher tensile strength with respect to traditionally reinforced segments.

21

505
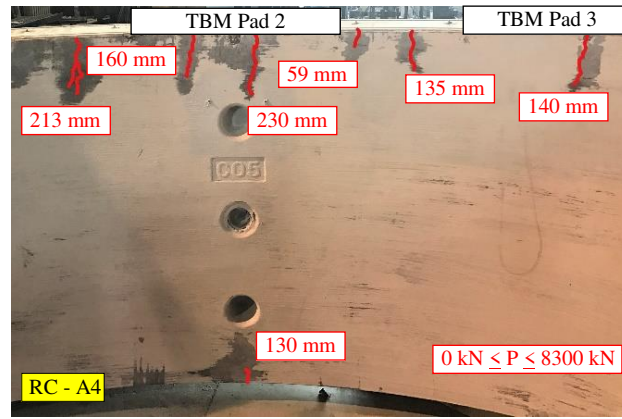
506
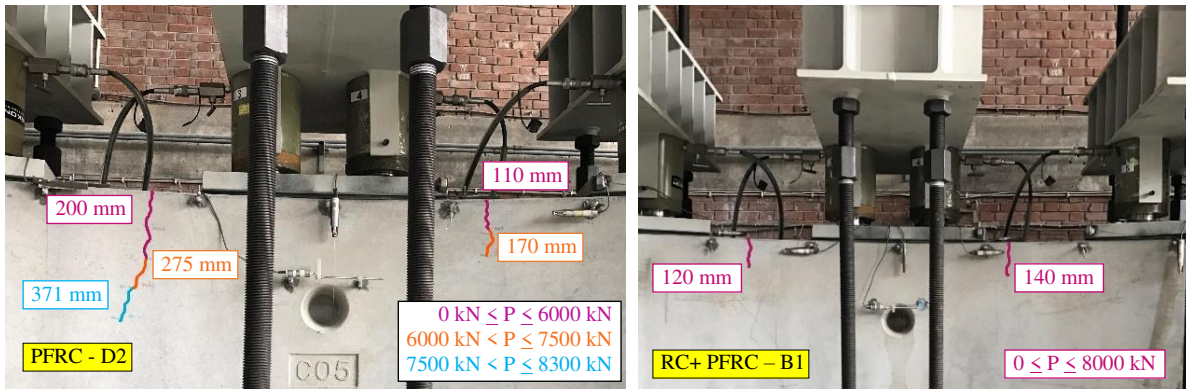
507   **Fig. 16.** Crack patterns and corresponding crack depths of test specimens.

508   **5. Conclusion**

509   The main purpose of this study was to evaluate the structural applicability of using macro-synthetic fibres in precast

510   tunnel segments by means of an experimental program on full-scale specimens. Accordingly, totally fourteen full-scale precast

511   tunnel segments of Mecidiyeköy - Mahmutbey metro tunnel characterized by four different reinforcement cases were studied

512   both under the flexure and point load test. The four different reinforcement solutions analysed were; typical conventional steel

513   reinforcement (RC); combination of polypropylene (PP) fibres and conventional reinforcement (RC + PFRC); the combination

514   of polypropylene and glass fibre reinforced polymer rebars (GFRP + PFRC); polypropylene fibres only (PFRC). Macro-

515   synthetic PP fibres with a 4 kg/m3 (Vf =0.44%) were adopted in hybrid cases, GFPP + PFRC and RC + PFRC segments, on

516   the other hand, the 6 kg/m3 (Vf =0.66%) were used for PFRC samples. Based on the experimental research, the following

517   conclusions can be highlighted:

518   -   Precast tunnel segments of the metro project can be reinforced either by the combination of glass fibre reinforced

519   polymer rebars and polypropylene fibres or by a combination of conventional reinforcement and polypropylene fibres

520   in case of satisfy the minimum criteria of project and codes. However, it should be noted that the conventional

521   reinforcement case (RC) guarantees a better structural performance when compared with the use of low volume

522   fraction of fibres. Although this study focuses on allowable serviceability crack width limit for tunnel segments, the

523   adopted fibre amounts are not suitable for significant post-cracking residual strengths. Preferred concrete matrix did

22

524   not meet the criteria of Model Code 2010 for both structural applications and using only PP fibres as minimum shear

525   reinforcement at ULS. If the aim is to improve the structural performance in addition to crack control, higher volume

526   fractions should be preferred;

527   -   Although PFRC specimens satisfy the design moment of the metro project when taken into account of initial crack

528   observation, the adopted quantity of PP fibres in the concrete mixtures did not significantly enhance both the flexural

529   capacity and the ductility of precast tunnel segments under flexure. They showed a low stiffer behaviour and post-

530   cracking softening under the flexure since they did not meet the minimum requirement of Model Code 2010;

531   -   PP fibres can partially increase both the flexural strength and the ductility under flexure in hybrid solutions of precast

532   tunnel segments; GFRP + PFRC and RC + PFRC. In fact, flexural test results of RC + PFRC solutions indicate that

533   the structure was able to develop multiple cracking. They also exhibited not only a considerable strength but also an

534   adequate ductility. While GFRP+PFRC showed a lower ductile behaviour compared to the classical hybrid case

535   because of the brittleness of the GFRP rebars. This may be caused due to the lower bond of GFRP rebars with respect

536   to the traditional steel ones and due to manufacturing lower quality of GFRP rebars than expected;

537   -   Under point load test, PP fibres both in case of PFRC and hybrid solutions (RC + PFRC and GFRP + PFRC) satisfied

538   the required structural performance at design TBM thrust load. The GFRP + PFRC exhibited suitable behaviour and

539   guaranteed a better cracking control ability compared to other solutions. In all specimens, the maximum crack widths,

540   even under high load level, were always lower than the allowable limit (0.3 mm).

541   In summary, full-scale test results revealed that combination of PP macro-synthetic fibres and GFRP rebars could be

542 an innovative reinforcement solution for precast tunnel segments in case of using a suitable quantity that satisfy the

543 requirements of projects and related codes. PFRC and GFRP + PFRC segments enable to fully exploit the advantages of MSFs

544 in terms of corrosion resistance in the presence of an aggressive surrounding environment, while the combination of PP fibres

545 with conventional steel reinforcement as a classical hybrid solution results in enhancing structural performance that could be

546 particularly effective in presence of aggressive conditions.

547   In spite of the achievements that were reported aforementioned, some issues regarding the topics presented in this

548 research still remain unclear. Even though the experimental results of alternative reinforcement solutions satisfy the design

549 values of MM metro project in terms of allowable crack width at serviceability limit, residual strength parameters are not

550 adequate in the tested specimens. More studies should focus on the optimisation of the quantity of both fibres and

551 reinforcements in precast tunnel segments in order to obtain more economic and durable solutions. In particular, finding suitable

552 fibre quantity and concrete mix design is significantly important to satisfy the minimum requirement of fib Model Code 2010

553 for fibre reinforced concrete segments, enhance the ductility of segments and obtain the post-cracking hardening behaviour.

554 Another important point is that carrying out many full-scale flexural tests is necessary to go deeper on a topic related to the

555 bearing capacity of hybrid solutions. In addition to serviceability limit state analysis, performing in-depth analysis to evaluate

556 the ultimate bearing capacity of alternative solutions of precast tunnel segments would be important to understand the general

23

557 structural behaviour of segments. Moreover, the fire resistance of alternative reinforcement solutions, especially their load-

558 carrying capacity during the fire event and after the fire, should be analysed experimentally like Yan et al., (2015). Although

559 shear force is not governing in design of FRC tunnel segments mostly, it is required to check the shear capacity of the tunnel

560 segments (ITA report n.16, 2016). Lastly, the long-term behaviour of precast segments under sustained loads should be

561 analysed, as well. These measures are significantly crucial for the safety of tunnel lining under extreme or unexpected

562 conditions.

563 **Acknowledgement**

568 **References**

569 Abbas, S., Nehdi, M.L., 2018. Mechanical behavior of RC and SFRC precast tunnel lining segments under chloride ions

570 exposure. J. Mater. Civ. Eng. 30, 1–13. https://doi.org/10.1061/(ASCE)MT.1943-5533.0002217

571 Abbas, S., Soliman, A.M., Nehdi, M.L., 2014a. Experimental study on settlement and punching behavior of full-scale RC and

572 SFRC precast tunnel lining segments. Eng. Struct. 72, 1–10. https://doi.org/10.1016/j.engstruct.2014.04.024

573 Abbas, S., Soliman, A.M., Nehdi, M.L., 2014b. Mechanical performance of reinforced concrete and steel fiber-reinforced

574 concrete precast tunnel lining segments: A case study. ACI Mater. J. 111, 501–510.

575 https://doi.org/10.14359/51687101

576 ACI Committee 440, 2015. Guide for the design and Construction of structural concrete reinforced with Fiber Reinforced

577 Polymer (FRP) bars ACI 440.1 R-15. American Concrete Institute.

578 ACI Committee 544, 2016. Report on design and construction of fiber-reinforced precast concrete tunnel segments ACI

579 544.7R-16. American Concrete Institute.

580 Almusallam, T.H., Al-Salloum, Y.A., 2006. Durability of GFRP rebars in concrete beams under sustained loads at severe

581 environments. J. Compos. Mater. 40 (7), 623–637.

582 ASTM, 2011. Standard test method for tensile properties of fiber reinforced polymer matrix composite bars. ASTM

583 D7205/D7205M-06, West Conshohocken, PA. https://doi.org/10.1520/D7205

584 Bakhshi, M., and Nasri, V. 2015. Design of segmental tunnel linings for serviceability limit state. In: ITA/AITES World Tunnel

585 Congress 2015 and 41st General Assembly, May 22–28, 2015. Lacroma Valamar Congress Center, Dubrovnik,

586 Croatia.

587 Beno, J., Hilar, M., 2013. Steel fibre reinforce concrete for tunnel lining - verification by extensive laboratory testing and
588   numerical modelling. Acta Polytech. 53, 329–337.

589 Caratelli, A., Meda, A., Rinaldi, Z., Romualdi, P., 2011. Structural behaviour of precast tunnel segments in fiber reinforced
590   concrete. Tunn. Undergr. Sp. Technol. 26, 284–291. https://doi.org/10.1016/j.tust.2010.10.003

591 Caratelli, A., Meda, A., Rinaldi, Z., 2012. Design according to MC2010 of a fibre-reinforced concrete tunnel in Monte Lirio,
592   Panama. Struct. Concr. 13, 166–173. https://doi.org/10.1002/suco.201100034

593 Caratelli, A., Meda, A., Rinaldi, Z., Spagnuolo, S., 2016. Precast tunnel segments with GFRP reinforcement. Tunn. Undergr.
594   Sp. Technol. 60, 10–20. https://doi.org/10.1016/j.tust.2016.07.011

595 Caratelli, A., Meda, A., Rinaldi, Z., Spagnuolo, S., Maddaluno, G., 2017. Optimization of GFRP reinforcement in precast
596   segments for metro tunnel lining. Compos. Struct. 181, 336–346. https://doi.org/10.1016/j.compstruct.2017.08.083

597 Conforti, A., Tiberti, G., Plizzari, G.A., 2016. Combined effect of high concentrated loads exerted by TBM hydraulic jacks.
598   Mag. Concr. Res. 68, 1122–1132. https://doi.org/10.1680/jmacr.15.00430

599 Conforti, A., Tiberti, G., Plizzari, G.A., Caratelli, A., Meda, A., 2017. Precast tunnel segments reinforced by macro-synthetic
600   fibers. Tunn. Undergr. Sp. Technol. 63, 1–11. https://doi.org/10.1016/j.tust.2016.12.005

601 Conforti, A., Trabucchi, I., Tiberti, G., Plizzari, G.A., Caratelli, A., Meda, A., 2019. Precast tunnel segments for metro tunnel
602   lining: A hybrid reinforcement solution using macro-synthetic fibers. Eng. Struct. 199, 109628.
603   https://doi.org/10.1016/j.engstruct.2019.109628

604 De la Fuente, A., Pujadas, P., Blanco, A., Aguado, A., 2012. Experiences in Barcelona with the use of fibres in segmental
605   linings. Tunn. Undergr. Sp. Technol. 27, 60–71. https://doi.org/10.1016/j.tust.2011.07.001

606 Demir, M., 2019. A method for the design of FRC tunnel linings reinforced with FRP bars. Master thesis, Middle East Technical
607   University, Ankara.

608 Di Carlo, F., Meda, A., Rinaldi, Z., 2016. Design procedure of precast fiber reinforced segments for tunnel lining construction.
609   Struct. Concr. 17 (5,1), 747–759.

610 EN 12390-3, 2009. Testing hardened concrete Part 3: Compressive strength of test specimens. European Standard.

611 EN 14651, 2005. Precast Concrete Products – Test Method for Metallic Fibre Concrete – Measuring the Flexural Tensile
612   Strength. European Standard.

613 EN 14889-2, 2006. Fibres for Concrete. Polymer Fibres. Definitions, Specifications and Conformity. European Standard.

614 EN 1992-1 1, 2004. Design of concrete structures - Part 1–1: General rules and rules for buildings. European Standard.

615 Fib Bulletins 65-66, 2012. Model code 2010: Final draft. Lausanne, Switzerland: International Federation for Structural
616   Concrete.

617 Gong, C., Ding, W., Mosalam, K.M., Günay, S., Soga, K., 2017. Comparison of the structural behavior of reinforced concrete
618   and steel fiber reinforced concrete tunnel segmental joints. Tunn. Undergr. Sp. Technol. 68, 38–57.
619   https://doi.org/10.1016/j.tust.2017.05.010

620   ISO 10406-1, 2008. Fibre-reinforced polymer (FRP) reinforcement of concrete – Test methods – Part 1: FRP bars and grids.

621   International Standard.

622   ITA report n. 16, 2016. Twenty years of FRC tunnel segments practice: lessons learnt and proposed design principles. April

623   2016, pp. 71, ISBN 978-2-970-1013-5-2.

624   ITATech report n. 7, 2016. Guidance for precast fibre reinforced concrete segments – vol. 1: design aspects. April 2016, pp.

625   47, ISBN 978-2-970-1013-2-1.

626   Liao, L., de la Fuente, A., Cavalaro, S., Aguado, A., 2015. Design of FRC tunnel segments considering the ductility

627   requirements of the Model Code 2010. Tunn. Undergr. Sp. Technol. 47, 200–210.

628   https://doi.org/10.1016/j.tust.2015.01.006

629   Luttikholt, A., 2007. Ultimate limit state analysis of a segmented tunnel lining. Master thesis, Delft University of Technology,

630   Delft, Netherlands.

631   Meda, A., Rinaldi, Z., Caratelli, A., Cignitti, F., 2016. Experimental investigation on precast tunnel segments under TBM thrust

632   action. Eng. Struct. 119, 174–185. https://doi.org/10.1016/j.engstruct.2016.03.049

633   Meda, A., Rinaldi, Z., Spagnuolo, S., De Rivaz, B., Giamundo, N., 2019. Hybrid precast tunnel segments in fiber reinforced

634   concrete with glass fiber reinforced bars. Tunn. Undergr. Sp. Technol. 86, 100–112.

635   https://doi.org/10.1016/j.tust.2019.01.016

636   Molins, C., Arnau, O., 2011. Experimental and analytical study of the structural response of segmental tunnel linings based on

637   an in situ loading test: Part 1: test configuration and execution. Tunn. Undergr. Space Technol. 26 (6), 764– 777.

638   Plizzari, G.A., Tiberti, G., 2007. Structural behaviour of SFRC tunnel segments. In: Proceedings of the 6th International

639   Conference on Fracture Mechanics of Concrete and Concrete Structures (FraMCos), vol. 3, pp. 1577–1584, ISBN

640   978-0- 415-44066-0.

641   Plizzari, G.A., Tiberti, G., 2008. Steel fibers as reinforcement for precast tunnel segments. Tunn. Undergr. Space Technol. 21

642   (3–4).

643   Spagnuolo, S., Meda, A., Rinaldi, Z., Nanni, A., 2017. Precast concrete tunnel segments with GFRP reinforcement. J. Compos.

644   Construct. ASCE 21 (5).

645   Tiberti, G., Conforti, A., Plizzari, G.A., 2015. Precast segments under TBM hydraulic jacks: Experimental investigation on the

646   local splitting behavior. Tunn. Undergr. Sp. Technol. 50, 438–450. https://doi:10.1016/j.tust.2015.08.013.

647   TS 708/2010, 2010. Steel for the reinforcement of concrete - Reinforcing steel, Turkish Standards Institution, Ankara, Turkey.

648   Yan, F., Lin, Z., Yang, M., 2016. Bond mechanism and bond strength of GFRP bars to concrete: A review. Compos. Part B 98,

649   56–69. https://doi.org/10.1016/j.compositesb.2016.04.068

650   Yan, Z.G., Shen, Y., Zhu, H.H., Li, X.J., Lu, Y., 2015. Experimental investigation of reinforced concrete and hybrid fibre

651   reinforced concrete shield tunnel segments subjected to elevated temperature. Fire Saf. J. 71, 86–99.

652   https://doi.org/10.1016/j.firesaf.2014.11.009

653   Yoo, D.Y., Kwon, K.Y., Park, J.J., Yoon, Y.S., 2015. Local bond-slip response of GFRP rebar in ultra-high-performance fiber-

654   reinforced concrete. Compos. Struct. 120, 53–64.